Journal of Bioenergetics and Biomembranes, Vol. 30, No. 5, 1998

Electron Tomography of Mitochondria from Brown Adipocytes Reveals Crista Junctions

G. A. Perkins,[1,2,5] J. Y. Song,[2] L. Tarsa,[2] T. J. Deerinck,[3,4] M. H. Ellisman,[3,4] and T. G. Frey[1]

Received July 14, 1998

Electron microscope tomography was used to examine the membrane topology of brown adipose tissue (BAT) mitochondria prepared by cryofixation or chemical fixation techniques. These mitochondria contain an uncoupling protein which results in the conversion of energy from electron transport into heat. The three-dimensional reconstructions of BAT mitochondria provided a view of the inner mitochondrial membrane different in important features from descriptions found in the literature. The work reported here provides new insight into BAT mitochondria architecture by identifying crista junctions, including multiple junctions connecting a crista to the same side of the inner boundary membrane, in a class of mitochondria that have no tubular cristae, but only lamellar cristae. Crista junctions were defined previously as the tubular membranes of relatively uniform diameter that connect a crista membrane with the inner boundary membrane. We have also found that the cristae architecture of cryofixed mitochondria, including crista junctions, is similar to that found in chemically fixed mitochondria, suggesting that this architecture is not a fixation artifact. The stacks of lamellar cristae extended through more of the BAT mitochondrial volume than did the cristae we observed in neuronal mitochondria. Hence, the inner membrane surface area was larger in the former. In chemically fixed mitochondria, contact sites were easily visualized because the outer and inner boundary membranes were separated by an 8 nm space. However, in cryofixed mitochondria almost all the outer membrane was observed to be in close contact with the inner boundary membrane.

KEY WORDS: BAT mitochondria; brown adipocytes; contact sites; crista junctions; cristae; cristae structure; electron microscopy; electron microscope tomography; mitochondria; mitochondrial structure.

INTRODUCTION

Brown adipose tissue (BAT) is a quantitatively important, although variable, thermogenic tissue that is activated by noradrenaline released at sympathetic nerve terminal in response to exposure to cold or to nutritional modifications (for a review, see Himms-Hagen, 1990). The thermogenic activity of BAT varies among species, age and environment, and is most active in the mammalian newborn. The high thermogenic capacity of BAT is due to an uncoupling protein (UCP) which occurs exclusively in mammalian brown adipocytes (for a review, see Klingenberg, 1993). The UCP is located principally in the cristae membranes (Loncar, 1990) and allows proton reentry into the mitochondrial matrix. This reentry bypasses the ATP synthase allowing for the dissipation of energy as heat and the development of high catabolic activity.

Our previous work with electron microscope tomography performed on neuronal mitochondria led

[1] Biology Department, San Diego State University, San Diego, California 92115.
[2] Department of Chemistry and Biochemistry, University of California San Diego, La Jolla, California 92093-0608.
[3] National Center for Microscopy and Imaging Research, University of California San Diego, La Jolla, California 92093-0608.
[4] Department of Neurosciences, University of California San Diego, La Jolla, California 92093-0608.
[5] Author to whom correspondence should be sent.

0145-479X/98/1000-0431$15.00/0

to the recognition of a mitochondrial structure, the *crista junction* (Perkins *et al.*, 1997a) that added to a new paradigm of cristae architecture (Mannella *et al.*, 1997). Crista junctions are the membranous connections between the crista membrane and the inner boundary membrane and encircle openings approximately 30 nm in diameter that are tubular and relatively uniform in size. Crista junction openings replace the view depicted in textbooks of broad openings into the intracristal space and suggests that there may be compartmentalization of inner membrane proteins between the contiguous inner boundary membrane and crista membrane.

On the basis of insights gained from electron tomographic reconstructions of liver (Mannella *et al.*, 1994, 1997) and neuronal (Perkins *et al.*, 1997a, b) mitochondria, which suggested that crista junctions might be a uniform structural principle, we hypothesize that this biomembrane junction is the governing architecture among all higher animals. To test this hypothesis, we reasoned that mitochondria with a prevalence of lamellar cristae are more likely to show infoldings of the inner membrane instead of crista junctions than are mitochondria with a prevalence of tubular cristae. Lea *et al.* (1994) used high-resolution scanning electron microscopy to determine that tubular cristae are commonly found in most cell types of higher animals with the exception of BAT mitochondria. They found that BAT mitochondria contain only "plate or shelflike" cristae and thus appeared to fit the conventional paradigm displayed in textbooks. Their technique, however, yielded only partial views of the internal structure. Therefore, there remained a need to visualize the complete three-dimensional (3-D) structure of BAT mitochondria at no less than 10 nm resolution to determine whether the cristae in BAT mitochondria formed crista junctions. Presently, only electron tomography offers this level of resolution for visualizing the internal structure of whole mitochondria. This paper presents evidence from both chemically fixed and cryofixed BAT that while the cristae all appear to be lamellar (cisternal), the crista junctions are all membranous tubes.

MATERIALS AND METHODS

Samples of interscapular BAT from 2 to 3-week-old rats were excised and prepared for electron microscopy using two different fixation protocols—cryofixation and chemical fixation. Cryofixation was performed by first anesthetizing the animal from which small BAT globules were taken from different interscapular regions. No pretrimming or slicing of the BAT was needed since the extracted tissue was small enough for good freezing (Hohenberg *et al.*, 1996). The tissue was subjected to impact-freezing against a polished copper block cooled by liquid nitrogen followed by freeze-substitution. The time required to remove the BAT and freeze it was no greater than 10–20 seconds, minimizing both the deleterious effects of anoxia on mitochondria and the autolytic processes that introduce structural changes to the tissue (Gunter *et al.*, 1994; Bakker *et al.*, 1995). The chemically fixed samples were prepared for electron tomography in the same manner described by Perkins *et al.* (1997a). One difference was the use of 2% potassium ferrocyanide to reduce osmium tetroxide in order to increase the contrast of membranes (Goglia *et al.*, 1992). Figure 1 is a flow chart of the specimen preparation procedures (left half) and of the tomographic procedures used indicating iterative steps and those steps requiring decisions based on observations. The image-processing routines involved in tomography (shown in the right half of Fig. 1) are described in greater detail by Perkins *et al.* (1997b), including a discussion of the relative uses of two reconstruction techniques: R-weighted backprojection and ART (algebraic reconstruction techniques).

RESULTS

Interscapular BAT can be identified by eye because of its small, globular brown mass surrounded by white adipose tissue. It can also be identified at the electron microscope level by its histological characteristics, which include multivacuolar lipid deposits, granular cytoplasm, roundish nuclei, and densely packed mitochondria (Zancanaro *et al.*, 1995). These mitochondria are juxtaposed to the lipid deposits and the nucleus. Figure 2a and b show low-magnification images taken from semithick sections of both cryofixed and chemically fixed BAT. The morphology is as described for projection images of preadipocytes or brown adipocytes (Goglia *et al.*, 1992). The high-magnification images (Fig. 2c and d) show representative mitochondria that were used for tomographic reconstructions made from single-axis tilt series acquired with an intermediate high-voltage electron microscope (400 kV). The tilt increment was 2° ranging from −60° to +60°. Three reconstructions of chemically fixed

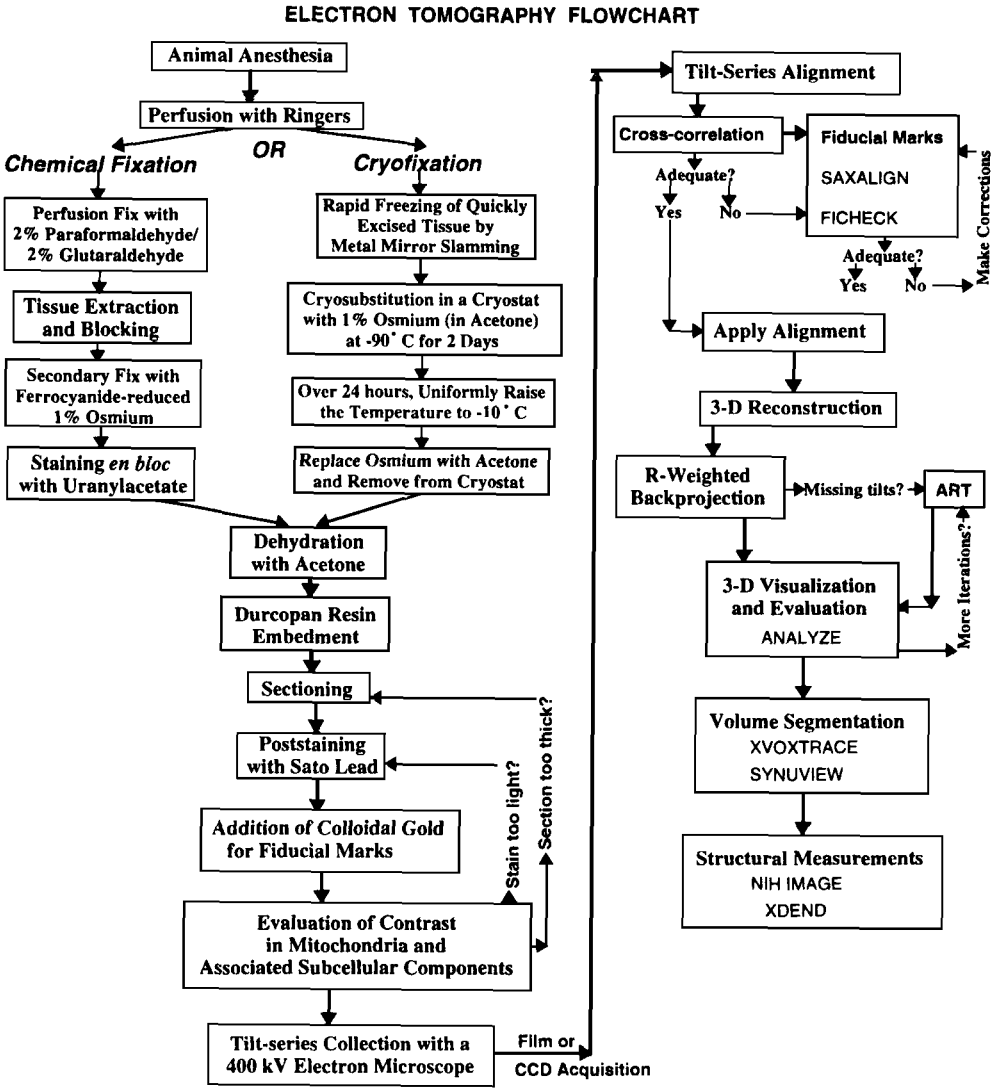

Fig. 1. Flow chart showing the tissue processing and electron microscopy steps (left-hand side) and computer image-processing steps (right-hand side) involved in obtaining and analyzing 3-D reconstructions of brown adipose tissue (BAT) mitochondria. Differences in preserving tissue by means of chemical fixation or cryofixation are emphasized. Those steps requiring evaluation and optimization of the specimen preparation technique (e.g., heavier poststain), or the improvement of the reconstruction (e.g., correcting the alignment), are indicated by branched paths. These steps sometimes require iterations as a normal part of the procedure. Computer programs are denoted by capital letters.

mitochondria from different animals were compared with each other and with three reconstructions of cryofixed mitochondria from one animal, but taken from different blocks of tissue. The mitochondrial ultrastructure appeared to be well preserved as indicated by the absence of swelling or membrane disruptions (Perkins *et al.*, 1997a), open intracristal space, and absence of scalloped edges along the mitochondrial perimeter (Dalen *et al.*, 1992a). We found close apposition between the outer and inner boundary membranes with no space observed between them. Whether the close apposition of outer and inner boundary membrane is a true structural characteristic or a feature of cryopreserved mitochondria is still controversial (Malhotra and Tewari, 1991; Dalen *et al.*, 1992b). We did not find that the matrix was significantly denser in the cryofixed mitochondria in contrast to the results of von Schack *et al.* (1993). Dalen *et al.* (1992a) reported

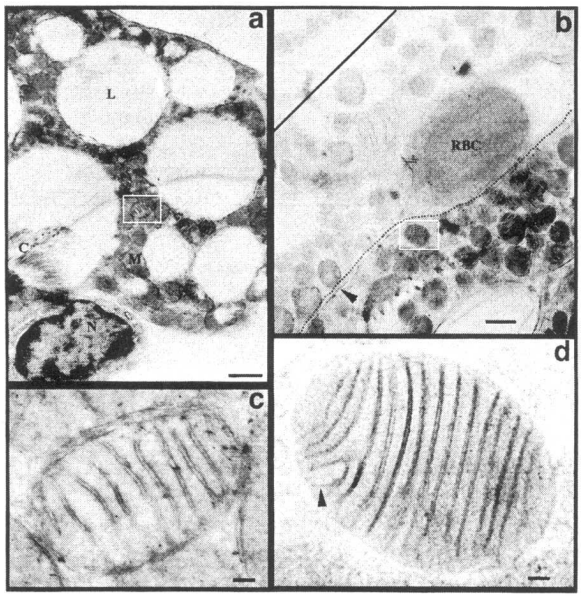

Fig. 2. Projection images of semithick sections (~0.5 μm) of brown adipose tissue (BAT) taken with an intermediate high-voltage electron microscope (400 kV). (a) Low-magnification image of a chemically fixed BAT specimen. Characteristic features of BAT are labeled: large lipid deposits, "L," roundish nuclei, "N," densely packed mitochondria, "M," and connective tissue, "C" dispersed throughout. The mitochondrion in the white box is shown magnified in (c) and was reconstructed using electron tomography. Scale bar = 1 μm. (b) Low-magnification image of a cryofixed BAT specimen. The freezing face, i.e., the surface that came into contact with the metal mirror kept at liquid nitrogen temperature, is indicated with a solid black line. The dotted black line demarcates the boundary of well-preserved mitochondria (occupying the lower right portion of the figure) and follows the contour of the cell membrane that can be visually followed from one end of the image to the other and is indicated at one point by an arrowhead. The region between these two lines (~6 μm across) shows poorly preserved mitochondria as evidenced by their grossly swollen matrix. The red blood cell found in this region is labeled "RBC." The mitochondrion in the white box is shown magnified in (d) and was reconstructed using electron tomography. Scale bar = 1 μm. (c) Image of a chemically fixed BAT mitochondrion. The black dots dispersed throughout the image are 10-nm colloidal gold clusters that were added to the section and were used as fiducial marks for aligning the tilt series. Note the easily visualized separation of the outer and inner boundary membranes (arrowhead). Scale bar = 100 nm. (d) Image of a cryofixed BAT mitochondrion. Note the granular cytoplasm that is also characteristic of this type of tissue. The cristae of BAT mitochondria are generally arrayed in stacks; one notable exception is marked with an arrowhead. The intracristal space is open. Scale bar = 100 nm.

a gradient of increasing cryodistortions with increasing distance from the "point of first impact," i.e., the tissue surface that comes in contact with the cold mirror during impact-freezing. We noticed changes in mitochondrial ultrastructure starting with partially collapsed intracristal space, then fully collapsed intracristal space, and finally progressing to scalloped mitochondrial periphery (presumably caused by microcrystals of ice formed by less-than-rapid freezing) in agreement with Dalen and co-workers.

We found that mitochondria with well-preserved ultrastructure occupied a narrow strip ~6–10 μm from the point of first impact. The reconstructed mitochondria analyzed here came from this strip and displayed the characteristics of well-preserved structure described above, except where noted. Unlike Dalen and co-workers, we discovered that mitochondria occupying positions ~0–6 μm from the point of first impact did not have the expected good structural features; this may have been caused by mechanical damage during dissection, such as disrupted cell membranes. Figure 2 shows a number of mitochondria in this strip that are grossly swollen, including some with no visible cristae. Furthermore, the presence of the red blood cell and the swollen appearance of the mitochondria argue that these cellular components "leaked" from damaged tissue coating the BAT surface. If the "liquid layer" that makes contact with the freezing mirror is too thick, good cryopreservation is prevented (Hohenberg *et al.*, 1996). However, the thickness did not appear to be too great for the mitochondria we reconstructed.

Electron tomography was used to examine the membrane topology of BAT mitochondria because it is presently the imaging technique (Perkins and Frey, 1997) that provides the highest 3-D resolution of the internal structure from thick sections of mitochondria (Mannella *et al.*, 1994, 1997; Frank, 1995; Perkins *et al.*, 1997a). Figure 3 shows sections through representative 3-D reconstructions of BAT mitochondria produced using electron tomography. Contact sites, first described by Hackenbrock (1968), were noted and their dimensions were measured for the three chemically fixed mitochondria, but not for the three cryofixed mitochondria. The latter displayed the inner boundary membrane in such close apposition to the outer membrane over most of the mitochondrial periphery that no space between them was resolved and discrete contact sites, as described by Perkins and co-workers, were not often observed. The cristae appear lamellar, as depicted in the literature, and crista junctions were observed, as shown by the inset in the lower right portion of Fig. 3a, which is an orthogonal view providing a cross section of a junction (boxed) showing its circular profile. The sections from which the mitochondria were reconstructed were ~0.2 μm thick for the

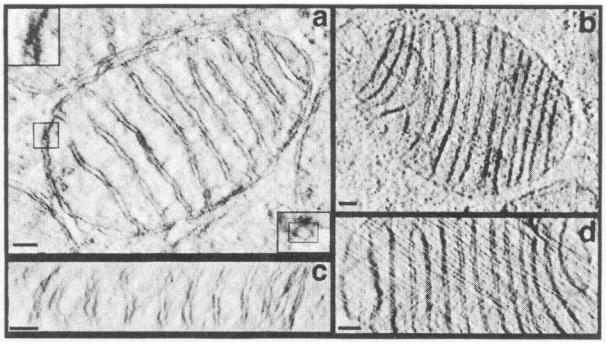

Fig. 3. Slices of 3-nm thickness through the 3-D reconstructions of the mitochondria shown in Fig. 2. (a) Slice through the reconstruction of the chemically fixed mitochondrion shown in the same orientation as in Fig. 2. An example of a contact site is boxed and shown magnified in the upper left-hand corner. An example of a crista junction, which was taken from a perpendicular view, is displayed in the box centered in the inset placed in the lower right-hand corner. Scale bar = 100 nm (b) Slice through the reconstruction of the cryofixed mitochondrion shown in the same orientation as in Fig. 2. Scale bar = 100 nm (c and d). Slices showing views perpendicular to those shown in (a and b), respectively, demonstrating the lamellar nature of the cristae found in BAT mitochondria. Scale bars = 100 nm.

chemically fixed mitochondrion and ~0.5 μm thick for the cryofixed mitochondrion, allowing one to visualize membrane topography through a substantial portion of the reconstructed mitochondrion. In the three reconstructions of chemically fixed mitochondria, the membranes had high contrast, which allowed us to easily follow their topology in 3-D. However, the membrane contrast in the three reconstructions of cryofixed mitochondria was lower, which may not be fully accounted for by the increased section thicknesses utilized for the cryopreparations; the lower contrast and fuzzier membranes may be due to the rapid freezing/freeze-substitution method employed. In contrast to neuronal mitochondria (Perkins *et al.*, 1997a), the cristae of BAT mitochondria were all lamellar; no tubular cristae were observed. However, the crista junctions were all narrow tubes, similar to those visualized in neuronal mitochondria. The side views (Fig. 3c and d) demonstrated that most of the lamellar cristae partition the reconstructed volume, although there were a few that did not; this is most evident in Fig. 3c. This view agrees with the description of Lea *et al.* (1994), except for their description of perforations in the cristae to maintain matrix continuity. Instead of perforations, we found that matrix continuity was maintained by large openings from one matrix space to the next, occurring adjacent to the inner boundary membrane (see Fig. 4c and d). This descriptive difference may be attributed to a difference in preparative techniques.

Figure 4 displays views of the segmented volumes of both cryofixed and chemically fixed BAT mitochondria. Segmentation is a visual tool that defines and dissects volume components and thus facilitates interpretation, measurement, and understanding of interrelationships of complex structures (Perkins *et al.*, 1997b). Although the cristae in BAT mitochondria were almost always lamellar, one exception is the crista of the cryofixed mitochondrion rendered in bluish-green (Fig. 4b and d), which is branched and has more curvature than the other cristae. The side views of Fig. 4 show that even mitochondrial types exhibiting only lamellar cristae, such as BAT mitochondria, nevertheless have membranous connections to the inner boundary membrane defined by discrete crista junctions. Lamellar cristae often had multiple crista junctions arrayed on the same side of the inner boundary membrane, e.g., Fig. 4c and d. Note that cristae in cryofixed specimens fill the mitochondrial cross section more completely than those in chemically fixed BAT mitochondria. This is most obvious in comparing the greenish-yellow and pink cristae in Fig. 4c, where there are large openings connecting the matrix spaces on either side of the cristae and the greenish-yellow and bluish-green cristae in Fig. 4d whose edges more closely follow the contour of the inner boundary membrane. Even in the cryofixed specimens, however, the openings connecting matrix spaces on either side of the cristae appear to be large enough that they would not provide a diffusion barrier from one matrix compartment to another. It is clear from Fig. 4 that BAT mitochondria display the same crista junction features we found in neuronal mitochondria. Whereas Fig. 4a–d provide an analytical view of the reconstructed membrane features, Fig. 4e and f was included to provide a more complete and aesthetic view of the density of cristae packing and the twists observed as the cristae ensemble traverses the mitochondrial volume. A wealth of information can be quickly taken in by rotating the completely segmented volumes. For example, when observing the edges of the cristae, it becomes apparent that there are many places where the crista membrane abuts the inner boundary membrane without forming a crista junction.

Measurements of the substructure dimensions of cryofixed and chemically fixed BAT mitochondria are compared to those of neuronal mitochondria in Fig. 5. The dimension of the crista junction opening in all three preparations was essentially the same. The mean

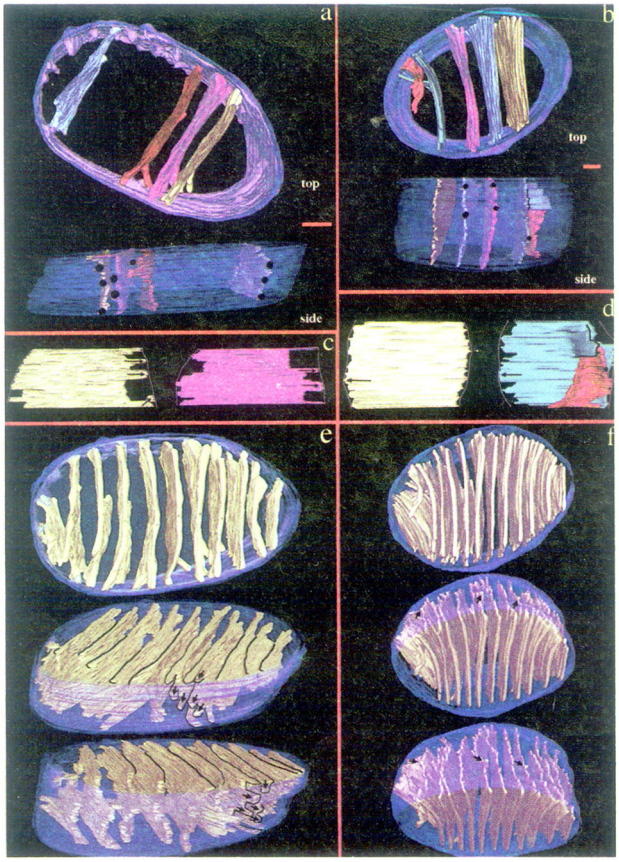

Fig. 4. Surface-rendered depictions of the 3-D reconstructions of Fig. 3 after the volumes were segmented by manually contouring the regions bounded by the outer, inner, and cristal membranes. Note that the inner boundary and cristal membranes are continuous surfaces but were segmented independently to highlight their separate topographies. Distinct cristae were segmented independently to examine membrane morphology and connectivity and are displayed using different colors. (a) Surface-rendered volume of a chemically fixed mitochondrion. Top: Four segmented cristae (out of 10 total) showing lamellar topology are displayed, as are the outer (dark blue) and inner boundary (light blue) membranes. The mitochondrion length (long axis) is ~850 nm. Side: The crista junction openings, which connect the intermembrane space with the intracristal space, are shown in black. The height of the segmented volume is ~200 nm and represents the portion of the volume that displayed clear features. Scale bar = 100 nm. The scale bar also applies to Fig. 4c and e. (b) Surface-rendered volume of a cryofixed mitochondrion. Top: Five segmented cristae (out of 16 total), showing lamellar and branched topology, are displayed. The outer and inner boundary membranes were not resolved in cryofixed specimens and, hence, were segmented together. The mitochondrion length is ~1000 nm Side: The crista junction openings are shown in black. The height of the segmented volume is ~480 nm. Scale bar = 100 nm. The scale bar also applies to Fig. 4d and f. (c) Perpendicular views of two of the cristae shown in (a). Crista junctions are indicated by arrows and the peripheral membranes by an orange curve. These views highlight the lamellar nature of BAT cristae and show the relatively large openings along the periphery that connect one matrix space with the next. (d) Perpendicular views of three of the cristae shown in (b). The bluish-green crista is branched and the smaller compartment (red) extends less than half of the length (top to bottom) of the major compartment. Crista junctions are indicated by arrows. (e, f) Views rotated about selected axes of the completely segmented volumes of the reconstructed mitochondria of (a) and (b), respectively, showing all the cristae in greenish-yellow. The peripheral membranes (in blue) were made translucent to be able to fully visualize the cristae. The same crista junctions emphasized in (c) and (d) are also demarcated by arrows to highlight the spatial relationship to adjacent cristae shown in different orientations. An additional junction is marked in (f) because of its prominence in the center of the image.

values for the OM–IM width (length from the outer edge of the mitochondrial outer membrane across the inner membrane) were uniform between chemically fixed BAT and neuronal mitochondria. However, the measured OM–IM widths in chemically fixed mitochondria differed substantially from the mean width measured in cryofixed BAT mitochondria. The OM–IM value of 17 nm for the cryofixed samples was not much more than the mean value of 14 nm for the contact width. The close apposition of outer and inner boundary membranes is often a distinguishing feature of the cryofixed mitochondria examined from different cells, including neurons (Perkins *et al.*, 1997b), cultured cardiac cells (Dalen *et al.*, 1992a), and yeast (Pfanner *et al.*, 1992). Malhotra and Tewari (1991) suggested that the process of chemical fixation may cause swelling of the intermembrane space pushing the outer membrane and inner boundary membrane somewhat apart. Whether the outer membrane and the inner boundary membrane are actually in contact *in vivo* cannot be determined by our techniques at this time. The values for the measured diameter of contact sites were similar for the chemically fixed BAT and neuronal mitochondria, although there was a greater variance in the neuronal measurements. Nevertheless, these values highlight the punctate nature of contact sites in chemically fixed mitochondria. The difference in mean values for the measurements of crista width (the distance from the outer edge of one of the apposed cristae membranes across the intracristal space to the outer edge of the other membrane) in BAT mitochondria (~25 nm) and neuronal mitochondria (~30 nm) reflects the sometimes larger diameters of tubular cristae found in neuronal mitochondria, but not in BAT mitochondria.

Dalen *et al.* (1992a) showed electron micrographs of cryofixed mitochondria with collapsed intracristal space, but reported no measurements of the crista width

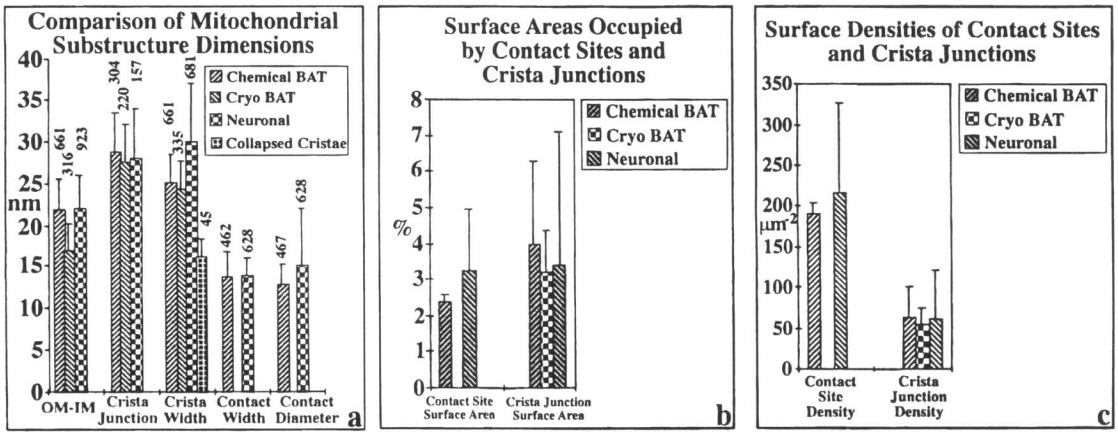

Fig. 5. Histograms comparing the measurements of the dimensions, surface areas and densities of selected substructures of BAT and neuronal mitochondria. Measurements were conducted on equally spaced slices through the reconstructed volumes (usually 40–90 slices per volume) using the program, NIH IMAGE. The various parameters were defined and visual examples were provided by Perkins *et al.* (1997a; see Fig. 2 and Table 2). (a) Mean values of the length measurements made from the 3-D reconstructions of three chemically fixed BAT mitochondria, three cryofixed BAT mitochondria, and five neuronal mitochondria (chemically fixed) of the five features displayed along the horizontal axis. The "contact width" was measured perpendicular to the membranes, from the outer edge of the outer membrane through to the inner edge of the inner membrane. The "contact diameter" was measured parallel to the membranes. "OM-IM" was measured perpendicular to the membranes, from the outer edge of the outer membrane through to the inner edge of the inner membrane at randomly selected points along the periphery that were not contact sites. "Crista junction" is the diameter measured across the bounding membranes at sites where the inner boundary membrane involutes into the interior. "Crista width" is the width across the bounding membranes at randomly selected points of cristae at sites other than junctions. The error bars indicate the standard deviations of the means, and the number over each bar is the number of measurements made. The mean value for the crista width of collapsed cristae was made from measurements of a cryofixed mitochondrial reconstruction. (b) Mean values and standard deviations of the surface areas occupied by contact sites and crista junction openings over the mitochondrial periphery as a percentage of the total surface area. (c) Mean values and standard deviations of the surface densities of contact sites and crista junctions expressed as the number per total surface area.

after collapse. Since a significant number of these collapsed cristae were "fuzzy," we were interested in comparing measurements of the collapsed crista width taken from their micrographs with measurements from one of our cryofixed BAT mitochondrial reconstructions showing the same kind of cryodistortion. Figure 6 displays an image and reconstruction slice of a cryofixed BAT mitochondrion from the strip where well-preserved mitochondria can be found and does not appear to be damaged by ice microcrystals (damage as indicated by "scalloped" edges), even though many of the cristae are shown to be collapsed. The mean crista width measured from sections through this reconstruction was 16 nm (Fig. 5), which was comparable to the values of 15 to 19 nm (the fuzzier cristae having the larger values) measured from the Dalen and co-workers micrographs. These values were similar to the OM-IM mean of 17 nm for cryofixed BAT mitochondria and distinct from the value of 25 nm obtained from both studies of uncollapsed cristae, and thus represent close apposition of the cristal membranes. The fuzzy appearance of the collapsed cristal membranes may be due to a loss of structural integrity of the constituent membrane and membrane-associated proteins.

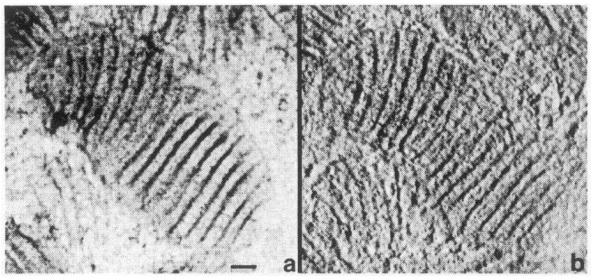

Fig. 6. (a) Electron micrograph of an untilted, cryofixed BAT mitochondrion and (b) slice through the center of its 3-D reconstruction showing collapsed cristae. Collapsed cristae are indicative of the cryodistortion found in cryofixed mitochondria that were not frozen as rapidly as needed to preserve the native structure. Measurements from ~40 slices contributed to the histogram values shown in Fig. 5a. Scale bar = 100 nm.

We compared the mean surface areas occupied by contact sites and crista junction openings from BAT mitochondria with the means obtained from neuronal mitochondria (Fig. 5b). The mean surface densities of these two structural features were also compared (Fig. 5c). It should be noted that the mean values between tissue types are similar, but that the variance is greater within the neuronal mitochondria measurements. The larger variance is due to the combining of data from dendritic and axonal mitochondria and data from mitochondria found in the peripheral nervous system (PNS) and central nervous system (CNS).

Using two different methods for measuring surface areas and volumes, we determined two ratios that further our understanding of the compartmentalization of mitochondria by way of cristae membranes. Table I displays the ratios of cristae surface area and cristae volume to mitochondrial volume made from (1) the tomographic volumes segmented according to the membrane topology and (2) projection images of thin sections. Scaling the cristae measurements by the mitochondrial volume appears to be the most appropriate mechanism for examining cristae compartmentalization because mitochondrial volume is proportional to mitochondrial mass for mitochondria in similar states. The upper portion of the table presents measurements using the program XDEND. This method has the advantage of accurate volume and surface area measurements as long as the segmentation was accurate. It has the disadvantage that measurements from the segmented mitochondrial volumes were necessarily sparse because of the extraordinary amount of time needed for segmentation. The lower portion of the table presents estimates of volume and surface area made from area and perimeter measurements, respectively, using the program NIH Image. The advantage of this method is that the population sampling can be scaled up by increasing the number of animals used to provide reasonable confidence levels for a statistical analysis. The disadvantage is that, unlike the XDEND measurements, these measurements are only estimates of the true metrics (volume and surface area). The

Table I. Ratios of Surface Area and Volume

Class of mitochondrion[a]	Cristae volume / mitochondrial volume[b]	Cristae surface / mitochondrial volume[c]
Segmented mitochondrial volumes		
Cryofixed BAT (1)	0.28	0.027 nm^{-1}
Chemically fixed BAT (1)	0.13	0.024 nm^{-1}
Neuronal (1)	0.11	0.015 nm^{-1}
Projection images of thin sections[d]		
Cryofixed BAT (20)	0.23 ± 0.040	0.024 ± 0.0035 nm^{-1}
Chemically fixed BAT (17)	0.22 ± 0.067	0.022 ± 0.0081 nm^{-1}
Neuronal (20)	0.17 ± 0.054	0.016 ± 0.0071 nm^{-1}
T-test on projection images[e]		
Cryofixed and neuronal	p = 0.00053	p = 0.00015
Chemically fixed and neuronal	0.0019	0.013
Chemically fixed and cryofixed	0.68	0.52
Confidence intervals on projection images[f]		
Cryofixed and neuronal	0.056 ± 0.045(99.5%)	0.0075 ± 0.0054(99.5%)
Chemically fixed and neuronal	0.051 ± 0.041(95%)	0.0062 ± 0.0051(95%)
Chemically fixed and cryofixed	0.0054 ± 0.031(90%)	0.0013 ± 0.0035(90%)

[a] The number in parentheses represents the number of distinct mitochondria used for the measurements. No mitochondria with collapsed cristae were used in this analysis.

[b] For the segmented mitochondrial volumes, the volume enclosed by all of the cristae membranes was measured and divided by the volume of the reconstructed mitochondrion. For the projection images of thin sections, the area enclosed by the outer membrane was measured and divided by the sum of the measured areas enclosed by the cristae.

[c] For the segmented mitochondrial volumes, the surface area of all the cristae membranes was divided by the mitochondrial volume. For the projection images of thin sections, the area enclosed by the outer membrane was divided by the sum of the measured cristae perimeters.

[d] Mean ± S. D. for the number of measurements in parentheses.

[e] Probability from a student's *t*-test assuming unequal variances and two-sided tales and tests whether two sample means are equal.

[f] Confidence intervals for the difference in means between the two samples; the values shown are difference in mean ± confidence limit. The significance level is provided in parentheses.

accuracy of the measurements is dependent on stereological principles, which strictly hold only for planar sections of negligible thickness. However, a commonly used rule of thumb is that if the section thickness is less than 1/10 the width of the object, a mitochondrion in this instance, then these estimates can be sufficiently accurate to allow for a statistical analysis. The section thickness for our thin sections ranged from 50 to 100 nm and with the observation that the mitochondria observed were on the order of 1 μm across, it is reasonable to apply the estimates for the metrics in Table I.

We used a student's *t*-test with the two metrics of Table I to determine if the descriptive differences in cristae topology observed by electron tomography are confirmed by a statistically defined difference in quantitative cristae volume and surface area between the populations of chemically fixed BAT, cryofixed BAT, and neuronal mitochondria. The *t*-test returned a probability value (*p*) for the equality of the means from two samples. We found that the *p* values were very low between neuronal and BAT mitochondria. These low values show that the sample means are unequal and strongly suggest that the underlying populations are different. These differences in cristae volume and surface area reflect the prevalence of tubular cristae in neuronal mitochondria and their absence in BAT mitochondria. Even though the *p* values were much higher for the comparison of chemically fixed and cryofixed BAT samples, we wondered if the sample means might be unequal. Hence, we computed the confidence intervals shown in Table I. The confidence intervals confirm unequal sample means between the BAT and neuronal mitochondria at high significance levels (95 and 99.5%). However, the hypothesis of equal means between the two BAT samples could not be rejected, thus suggesting that the cristae topology is similar whether chemically fixed or cryofixed.

DISCUSSION

The discovery that *only* crista junctions, can be found in a class of mitochondria (BAT) that exhibit *no* tubular cristae, but instead have only large lamellar cristae, supports the new paradigm of the structure of the mitochondrial inner membrane (Mannella *et al.*, 1997; Perkins *et al.*, 1997a) in place of the common depiction seen in textbooks. We have analyzed the reconstructions of six BAT mitochondria, which provided a view different in important structural aspects from descriptions of BAT mitochondria found in the literature (e.g., Lea *et al.*, 1994), yet in some ways similar to the neuronal mitochondria we examined previously (Perkins *et al.*, 1997a). The similar features include the close apposition of the inner boundary and outer membranes, which come together at discrete contact sites 14 nm in diameter and tubular 30-nm diameter crista junctions connecting the inner boundary membrane to the crista membrane. Although neuronal mitochondria contain both large lamellar cristae and tubular cristae, mitochondria from both chemically fixed and cryofixed brown adipose tissue have cristae that were all large, closed lamellar structures; no tubular cristae were observed. However, the crista junctions were all narrow tubes, similar to those visualized in neuronal mitochondria.

The improved 3-D information afforded by electron microscope tomography (Perkins *et al.*, 1997b) was the key to a new understanding of the complexity of the membrane topology in mitochondria. We have extended our previous work on mitochondrial membrane structures by: (1) Identifying crista junctions with the same structure and dimensions, including multiple junctions connecting a crista to the same side of the inner boundary membrane, in mitochondria outside the brain and PNS. This observation is consistent with our hypothesis that during growth or development, cristae are initialized ("bud") from these junctions and merge into a lamellar compartment. (2) Confirming the punctate nature of contact sites in chemically fixed mitochondria. However, in cryofixed mitochondria almost all the outer membrane is in close contact with the inner boundary membrane. (3) Finding no network of merging tubular cristae in BAT mitochondria, in contrast to the membrane tubes merging to form lamellae observed in neuronal mitochondria. (4) Demonstrating the capability to measure surface areas and volumes of segmented reconstructions with the new program XDEND.

Recent interest in the possibility of structural artifacts in chemically fixed mitochondria imaged *in situ* (von Schack *et al.*, 1993) motivated us to perform electron tomography on cryofixed BAT mitochondria. In particular, we wished to compare the structures of cryofixed mitochondria with chemically fixed mitochondria to determine if the new cristae paradigm observed in neuronal mitochondria was a result of the chemical fixation procedure. We found that the basic cristae architecture of cryofixed mitochondria is the same as that found in chemically fixed mitochondria, suggesting that while no fixation procedure is completely free of artifacts, this architectural feature is

likely found *in vivo*. The relatively high resolution afforded by the powerful 3-D imaging tool of electron tomography (Perkins and Frey, 1997) allowed us to measure and compare the dimensions of mitochondrial fine structure in cryofixed and chemically fixed mitochondria. The similar dimensions measured for the cristae features preserved with the different fixation techniques attests to the validity of these features and confirms a view of mitochondrial compartmentalization that differs from previous models. However, the difference in the measured OM-IM width lends a cautionary note to the visualization and interpretation of contact sites. The close apposition of the outer membrane and inner boundary membrane over essentially all the periphery in cryofixed mitochondria may imply that, *in vivo*, contact sites are more extensive than indicated in chemically fixed mitochondria. Alternatively, loss of the intermembrane space may be a cryofixation artifact. Unfixed rat liver tissue rapidly frozen on a liquid helium-cooled copper block and freeze-fracture replica labeled had mitochondria with what appeared to be separated outer and inner boundary membranes (Fujimoto *et al.*, 1996). The separation, however, was difficult to measure because of the metal shadowing employed in this technique.

It has yet to be determined if the matrix components are preserved to the same extent in the cryo approach as with the chemical approach; i.e., could there be a differential loss of matrix proteins and/or DNA depending on the approach used? This question arises when comparing electron micrographs of the same type of mitochondrion fixed with glutaraldehyde or cryofixed, e.g., in the cultured cardiac cells of Dalen *et al.* (1992a). Their glutaraldehyde-fixed mitochondria displayed a much darker matrix than did their cryofixed mitochondria. A darker matrix is generally believed to indicate that more of its constituents are present. In contrast, our BAT mitochondria displayed about the same level of matrix contrast whether cryo or chemically fixed. The difference in the results obtained by Dalen and co-workers and by us may be attributed to the different fixatives used. Our experiments with a combination of paraformaldehyde/glutaraldehyde and ferrocyanide-osmium tetroxide resulted in high contrast of the mitochondrial membranes in comparison to the matrix. To understand the difference in matrix contrast reported by Dalen and co-workers, it should be noted that the lighter matrix produced by cryofixation may indicate that matrix elements have been removed, or it may simply reflect the reactive preference of OsO_4 in a nonaqueous environment. In addition, it has been well documented that straight glutaraldehyde fixation results in a well-fixed matrix that upon staining can be so dark as to obscure the membranes (Glauert, 1975). Thus, careful consideration must be taken to choose the fixation procedure (whether chemical or cryo) that might best preserve the mitochondrial components of interest.

In comparing the structures of chemically fixed neuronal mitochondria and BAT mitochondria, a number of similarities stand out which may be significant for mitochondrial biogenesis. The outer and inner boundary membranes are far enough apart to reveal discrete contact sites holding the two together. In both types of mitochondria, the inner boundary membrane invaginates at numerous sites, crista junctions, which are tubular and relatively uniform in diameter. In neuronal mitochondria, however, the tubular structure of the crista junctions often persists to the extent that some crista are entirely tubular while other tubular cristae merge to form lamellar cristae. We speculate that this difference might result from the larger surface area of cristae membrane in BAT mitochondria than in neuronal mitochondria, and given a similar density of crista junctions, this increased surface area is accommodated by forming only large lamellar cristae. One important point to note is that this increase in cristae surface area does not cause an increase in the diameter of the crista junctions. The uniform size and shape of crista junctions between two mitochondria types with different cristae morphologies suggests that there may be some components that cause their formation and stabilize their structure. This leads to the hypothesis that cristae begin by a budding of the inner boundary membrane at crista junctions and grow by the addition of membrane components, perhaps at the junction site, causing tubular cristae to grow longer and eventually merge with other cristae to form large lamellar compartments.

The occurrence of stacks of lamellar cristae with no tubular cristae present may be influenced by the unique bioenergetics of BAT mitochondria. The stacks of lamellar cristae extended through more of the BAT mitochondrial volume than did the lamellar cristae found in neuronal mitochondria (Perkins *et al.*, 1997a). Hence, the inner membrane surface area was significantly larger in the BAT mitochondria (Table I), which may reflect an increase in proteins involved in the electron transport chain along with the additional surface occupied by the UCP's. This is consistent with the high metabolic/thermogenic activity of this type of mitochondrion. Densely packed cristae is a feature

of mitochondria in tissues with high metabolic demands, such as heart muscle (Jacob *et al.*, 1994; Ruiz-Lozano *et al.*, 1997), and is thought to reflect a high capacity for ATP production.

The hypothesis of the existence of both stable and labile contact sites (van der Klei *et al.*, 1994) can be speculated upon by a comparison of cryofixed and chemically fixed mitochondria. From the results reported here, it now appears that for mitochondria in the orthodox conformation, contact site parameters might be relatively uniform between tissue types, based on the limited comparison of data from dendritic/axonal, CNS/PNS, and BAT mitochondria prepared with slightly different chemical fixation procedures. With cryofixed mitochondria, the outer and inner boundary membranes are closely apposed over almost their entire surfaces, preventing a comparison of contact site dimensions. If not a cryofixation artifact, this extensive contact may reflect a natural capacity of the two membrane systems to create transient (dynamic), labile contact sites (Pfanner *et al.*, 1992) that may play different roles (as reviewed in Perkins et al., 1997a).

On the other hand, the punctate contact sites, which occupy much less surface area (mean ~2–3%, Fig. 5b) in chemically fixed mitochondria, may represent stable contact sites that hold the two membranes together during fixation. Malhotra and Tewari (1991) hypothesized that osmotic pressure, which may occur during the finite time required for fixation, might cause a slight swelling of the intermembrane space separating the outer and inner boundary membranes. If functional transient contact sites exist, then this relatively minor swelling of the intermembrane space could disrupt them leaving stabile contact sites intact. The putative stable contacts may serve a structural as well as functional purpose by holding the outer and inner membranes together.

This speculation of stable and labile contact sites has import not only to the understanding of the dynamics of protein and ATP/ADP traffic across the mitochondrial membranes, but also in defining the conditions for specimen preparation and characteristic morphology that will allow for the reliable study of different classes of contact sites. For example, it was suggested that contact sites should be defined only in condensed mitochondria characterized by a reduced matrix volume and a greater separation between the outer membrane and inner boundary membrane at the contact sites (van der Klei *et al.*, 1994). However, it now appears that the condensed state is probably not a physiological state (e.g., observed with purified mitochondria but not generally observed with mitochondria *in situ*; Mannella *et al.*, 1994). The work reported here allows for the study of the putative stable and labile contact sites under well-defined preservation of *in situ* mitochondria that are not condensed but rather are orthodox. Strengthening the hypothesis of stable contact sites and determining their 3-D distribution and composition might be accomplished in chemically fixed mitochondria through a combination of labeling, e.g., with antibodies and electron tomography. Conversely, the possibility of labile contact sites might best be investigated by labeling of mitochondria in cryofixed specimens that do not show evidence of cryoartifacts or ice damage as manifest by a scalloped periphery or collapsed cristae.

In conclusion, by comparing the fine structure of mitochondria preserved by cryofixation or chemical fixation, confidence in the membrane architecture observed in both fixation procedures is increased. This work modifies previous conceptions of the membrane architecture of BAT mitochondria by identifying the presence of crista junctions. Contact sites were easily visualized in chemically fixed mitochondria because of the slight separation of outer and inner boundary membranes, but were not observable in cryofixed samples because of the close apposition of these membranes. The implication of the ability to observe these sites is discussed in the context of the still controversial concept of stable and labile contact sites.

ACKNOWLEDGMENTS

We are grateful for the new image processing and measurement programs created by Steve Lamont and for advice on statistical interpretation of measurements by Steve Young. This work was supported in part by grants from the American Heart Association, CA Affiliate grant #95-301 and Western States Affiliate grant #98-256A to T. G. Frey, and from the National Science Foundation (ASC 93-18180) and the National Institutes of Health, National Center for Research Resources (RR 04050) to M. H. Ellisman.

REFERENCES

Bakker, A., Goossens, F., De Bie, M., Bernaert, I., van Belle, H., and Jacob, W. (1995). *Histol. Histopathol.* **10**, 405–416.

Dalen, H., Lieberman, M., LeFurgey, A., Scheie, P., and Sommer, J. R. (1992a). *J. Microsc.* **168**, 259–273.

Dalen, H., Scheif, P., Nassar, R., High, T., Scherer, B., Taylor, I., Wallace, N. R., and Sommer, J. R. (1992b). *J. Microsc.* **165**, 239–254.
Frank, J. (1995). *Curr. Op. Struc. Biol.* **5**, 194–201.
Fujimoto, K, Umeda, M., and Fujimoto, T. (1996). *J. Cell Sci.* **109**, 2453–2460.
Glauert, A. M. (1975). *Fixation, Dehydration and Embedding of Biological Specimens*. North-Holland, Amsterdam.
Goglia, F., Geloen, A., Lanni, A., Minaire, Y., and Bukowiecki, L. J. (1992). *Am. J. Physiol.* **262**, C1018–1023.
Gunter, T. E., Gunter, K. K., Shew, S. S., and Gavin, C. E. (1994). *Am. J. Physiol.* **267**, C313–339.
Hackenbrock, C. R. (1968). *Proc. Natl. Acad. Sci. U.S.* **61**, 598–605.
Himms-Hagen, J. (1990). In *Thermoregulation: Physiology and Biochemistry* (Schonbaum, E. and Lomax, P., eds.), Pergamon Press, New York, pp. 327–414.
Hohenberg, H., Tobler, M., and Muller, M. (1996). *J. Microsc.* **183**, 133–139.
Jacob, W., Bakker, A., Hertsens, R. C., and Biermans, W. (1994). *Microsc. Res. Techn.* **27**, 307–318.
Klingenberg, M. (1993). *J. Bioener. Biomembr.* **25**, 447–457.
Lea, P. J., Temkin, R. J., Freeman, K. B., Mitchell, G. A., and Robinson, B. H. (1994). *Microsc. Res. Techn.* **27**, 269–277.
Loncar, D. (1990). *J. Struct. Biol.* **105**, 133–145.
Malhotra, S. K., and Tewari, J. P. (1991). *Cytobios* **68**, 91–94.
Mannella, C. A., Marko, M., Penczek, P., Barnard, D., and Frank, J. (1994). *Microsc. Res. Techn.* **27**, 278–283.
Mannella, C. A., Marko, M., and Buttle, K. (1997). *TIBS* **22**, 37–38.
Perkins, G. and Frey, T. (1999) In *Encyclopedia of Molecular Biology* (Creighton, T., ed.), in press.
Perkins, G., Renken, C., Martone, M. E., Young, S. J. Ellisman, M., and Frey, T. (1997a). *J. Struct. Biol.* **119**, 160–172.
Perkins, G., Young, S., Renken, C., Song, J. Y., Lamont, S., Martone, M., Lindsey, S., Frey, T., and Ellisman, M. (1997b). *J. Struct. Biol.* **120**, 219–227.
Pfanner, N., Rassow, J., van der Klei, I. J., and Neupert, W. (1992). *Cell* **68**, 999–1002.
Ruiz-Lozano, P., Smith, S. M., Perkins, G., Kubalek, S. W., Kelly, D. P., Boss, G. R., Sucov, H. M., Evans, R. M., and Chien, K. R. (1997). *Development* **125**, 533–544.
van der Klei, I. J., Veenhuis, M., and Neupert, W. (1994). *Microsc. Res. Techn.* **27**, 284–293.
von Schack, M. L., Fakan, S., Villiger, W., and Muller, M. (1993). *Eur. J. Histochem.* **37**, 5–18.
Zancanaro, C., Carnielli, V. P., Moretti, C., Benati, D., and Gamba, P. (1995). *Tissue Cell* **27**, 339–348.